

Aerodynamic Study Of Composite Ti-MMC Functionally Graded Grid Fins

Srikar Doddi¹, Dr. Kalpana J Ph D²

¹Dept of Mechanical Engineering

²Assist. Professor, Dept of Mechanical Engineering

^{1,2}Sanketika Vidya Parishad Engineering College

Abstract- Reusable rockets employ grid fins for descent control, but conventional materials fail under combined aerodynamic, structural, and thermal loads. This study evaluates Aluminium 7075-T6, Titanium Ti-6Al-4V, and Titanium Metal Matrix Composite Functionally Graded Materials (Ti-MMC FGMs) across Mach 0.8, 1.2, and 2.0 using a multi-physics ANSYS framework. Results show Ti-MMC FGMs provide up to 22% higher drag, 35% lower stresses, and 30% reduced deformation compared to titanium, while sustaining thermal stability beyond 2000 K. These findings establish Ti-MMC FGMs as superior candidates for reusable grid fins in next-generation aerospace systems

Keywords- Computational Fluid Dynamics, Finite Element Analysis, Metal Matrix Composite, Functionally Graded Material, Grid Fin, Lattice Fin, Drag Force, Lift Force.

I. INTRODUCTION

The development of Reusable Launch Vehicles (RLVs) has transformed spaceflight economics by enabling boosters to return safely and be flown multiple times. Unlike expendable systems, RLVs demand precise aerodynamic control during descent, particularly in the terminal landing phase where stability against pitch, yaw, and roll disturbances is critical. In this context, grid fins, also known as lattice fins, have emerged as essential aerodynamic control devices due to their ability to provide stabilization, control authority, and drag-based braking across a wide Mach spectrum.

Historically, grid fins were first studied in the 1950s by Sergey Belotserkovsky's team and later applied in Soviet escape systems, missiles such as the R-77, and U.S. munitions like the MOAB. Their modern relevance surged with SpaceX's Falcon 9 (Fig 1.1), where grid fins enable controlled re-entry and pinpoint booster landings. Compared to planar fins, grid fins offer compact stowability, predictable performance in transonic regimes, and superior drag generation, though at the cost of increased complexity and drag penalties during ascent.

The aerodynamics of grid fins are highly nonlinear. In subsonic flow, they act as modest drag brakes, while in the transonic regime ($0.8 < M < 1.2$), shock-boundary layer interactions dominate, causing sharp drag rises and nonlinear lift behaviour. At supersonic speeds ($M > 1.2$), strong bow shocks and vortex shedding enhance drag while maintaining flow stability. Their efficiency, however, is fundamentally linked to the material properties of the fins, which must endure coupled aerodynamic, structural, and thermal loads.

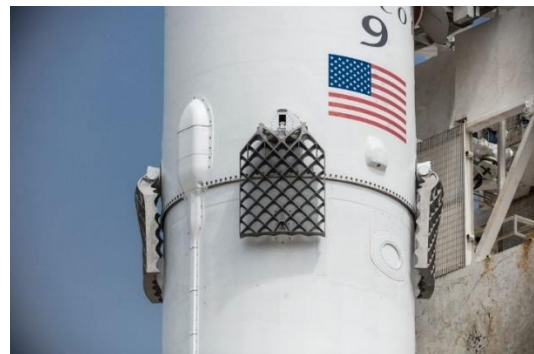


Fig 1.1 SpaceX Falcon9 Reusable Launch Vehicle Equipped with Grid Fins [Ref 32]

Existing materials suffer trade-offs. Aluminium alloys (e.g., 7075-T6) are lightweight and economical but fail under re-entry heating (~ 660 °C). Titanium alloys (e.g., Ti-6Al-4V), used on Falcon 9, provide higher strength and thermal resistance (~ 1600 °C) but are costly and difficult to manufacture in lattice geometries. Stainless steel offers durability and thermal stability but introduces prohibitive mass penalties. Carbon composites, though lightweight, degrade above ~ 600 °C and are unsuitable for re-entry. Thus, no conventional material simultaneously satisfies requirements of low weight, high thermal survivability, and cost-effectiveness.

To address this limitation, Titanium-based Metal Matrix Composites (Ti-MMCs) reinforced with ceramics such as SiC or Al₂O₃ have been explored. These composites improve stiffness, creep resistance, and high-temperature performance beyond monolithic titanium. Further, when designed as Functionally Graded Materials (FGMs), the ceramic reinforcement varies across the fin thickness—outer

ceramic-rich layers resist re-entry heating, while titanium-rich cores provide toughness and ductility. This gradation mitigates thermal stresses, delays crack initiation, and enhances fatigue life under repeated heating cycles.

While MMCs and FGMs have been studied for aerospace components such as turbine blades and heat shields, their application in aerodynamic control surfaces remains unexplored. This study introduces Ti-MMC FGMs for reusable rocket grid fins, combining the lightweight efficiency of aluminium, the strength of titanium, and the thermal resilience of ceramics. Through a multi-physics simulation framework in ANSYS, encompassing CFD, structural, and thermal analyses at Mach 0.8, 1.2, and 2.0, this work benchmarks Aluminium 7075-T6, Ti-6Al-4V, and Ti-MMC FGMs, demonstrating the superior performance of the proposed composite.

II. LITERATURE REVIEW

Aerodynamic Characteristics of Grid Fins:

Grid fins, initially developed for missile control, have become critical in reusable rocket systems due to their ability to retain control authority across a wide Mach range. Unlike planar fins, grid fins generate high drag while sustaining stability, making them effective during terminal descent. Numerical investigations confirm that lattice geometry strongly influences aerodynamic efficiency. For example, Faza et al. (2018) showed that swept angles alter lift-drag characteristics, while Dol (2021) reported that lattice thickness and chord ratio directly affect drag, with thicker webs increasing resistance but also structural loads. Aeroelastic effects are equally important; Huang et al. (2017) demonstrated that fin deformation can modify aerodynamic coefficients, emphasizing the need for coupled aero-structural analysis.

Planar vs. Grid Fin Comparisons:

While planar fins are efficient in subsonic flow, their effectiveness diminishes in transonic regimes due to early separation and reduced predictability. Grid fins, by contrast, maintain higher control forces and delayed separation at supersonic speeds. Tripathi et al. (2018) compared planar and grid configurations and confirmed the superior performance of grid fins beyond Mach 1.0. Industrial validation comes from Falcon 9 boosters, which employ titanium grid fins for precise re-entry control, while patents such as Jia et al. (2018) highlight their application in reusable rocket recovery.

Materials in Grid Fin Applications:

Material choice remains a central challenge in grid fin design. Aluminium alloys (e.g., 7075-T6) are lightweight and cost-effective but fail thermally at ~660 °C. Titanium alloys (e.g., Ti-6Al-4V) offer higher strength, fatigue resistance, and thermal tolerance up to ~1600 °C but are costly and difficult to manufacture in lattice geometries. Stainless steels, recently explored in SpaceX Starship prototypes, provide durability but add nearly double the mass of titanium, limiting ascent efficiency. Carbon fibre composites, though attractive for weight reduction, degrade above ~600 °C and cannot survive re-entry. This persistent trade-off between weight, thermal survivability, and cost limits current designs.

Advances in MMCs and FGMs:

Recent aerospace research has explored Metal Matrix Composites (MMCs) and Functionally Graded Materials (FGMs) as alternatives to monolithic metals. Titanium-based MMCs reinforced with ceramics such as SiC or TiB₂ exhibit superior stiffness-to-weight ratios, creep resistance, and fatigue performance. FGMs, first introduced by Koizumi (1993), gradually vary composition across thickness, reducing stress concentrations under steep thermal gradients. Studies by Birman and Byrd (2007) and Neville (2005) highlighted their effectiveness in high-temperature applications like turbine blades and re-entry shields. However, their potential in aerodynamic control surfaces such as grid fins remains unexplored.

Research Gap:

The literature establishes that while the aerodynamic benefits of grid fins are well understood, integrated studies considering aerodynamics, structural stresses, and thermal survivability are limited. Conventional materials—aluminium, titanium, steel, and carbon composites—each fail to meet all operational demands simultaneously. In contrast, Ti-MMC FGMs combine lightweight efficiency, structural strength, and superior thermal endurance, yet their application in grid fins has not been investigated.

The present work addresses this gap by:

- Proposing Ti-MMC FGMs as a new class of materials for reusable rocket grid fins.
- Performing comparative benchmarking against aluminium and titanium.
- Implementing a multi-physics simulation framework (CFD, FEA, thermal analysis) to replicate realistic re-entry conditions.

III. METHODOLOGY

Problem Statement:

The main challenge in reusable rocket grid fin design is achieving high aerodynamic control authority while ensuring structural strength and thermal survivability during re-entry. Conventional materials such as aluminium, titanium, and steel each present limitations in thermal resistance, manufacturability, or weight penalties. This study proposes Titanium Metal Matrix Composites with Functional Gradation (Ti-MMC FGMs) as a novel alternative and develops a multi-physics computational framework to evaluate their performance compared to aluminium and titanium alloys.

Research Workflow:

1. Geometry Modelling: A 3D grid fin model was created in CATIA V5 with key parameters (span = 750 mm, chord = 118 mm, lattice thickness = 5 mm) and exported in STEP format.
2. Material Assignment: Three materials were defined — Aluminium 7075-T6, Ti-6Al-4V, and Ti-MMC FGM with ceramic reinforcement.
3. Meshing: A hybrid mesh of tetrahedral unstructured cells and boundary layer inflation was generated to capture sharp lattice intersections and near-wall turbulence ($y^+ < 1$).
4. CFD Analysis: Mach 0.8, 1.2, and 2.0 cases were simulated in ANSYS Fluent (density-based solver, $k-\omega$ SST turbulence model). Drag and lift coefficients, pressure distributions, and shock structures were extracted.
5. Structural Analysis: Aerodynamic pressures from CFD were mapped as surface loads in Static Structural analysis to compute equivalent stresses, deformations, and safety factors.
6. Thermal Analysis: Convective heat flux profiles derived from CFD stagnation conditions were applied to assess re-entry thermal survivability.
7. Comparative Evaluation: Results were benchmarked across materials for aerodynamic efficiency, mechanical performance, and thermal endurance.

Geometric Parameters:

The fin configuration was based on un-swept lattice fins with blunt leading and trailing edges. Table 1.1 summarizes the primary physical parameters. These parameters ensure realistic aerodynamic scaling and structural fidelity.

Parameter	Value (mm)	Description
Rocket diameter (D)	1000	Base diameter
Fin span (s)	750	Radial projection
Fin width (b)	333.3	Overall width
Chord (c)	118	Axial dimension
Lattice thickness (t)	5	Strut wall thickness
Lattice cell length (a)	112.9	Inner cell spacing

Table 1.1 Physical Parameters of Grid Fin

Material Modelling:

Three materials were defined in ANSYS Engineering Data with their thermo-mechanical properties (Table 4.2):

1. Aluminium 7075-T6: Density = 2.8 g/cm³, Yield strength = 503 MPa, Melting point = 660 °C. Lightweight but unsuitable for re-entry heating.
2. Ti-6Al-4V: Density = 4.43 g/cm³, Yield strength = 880–950 MPa, Melting point = 1660 °C. Industrial standard for reusable grid fins but costly and heavy.
3. Ti-MMC FGM (Proposed): Titanium matrix reinforced with SiC particulates. Outer layers: 25% SiC (thermal resistance), inner layers: 5% SiC (ductility). Effective yield strength = 1000–1200 MPa, thermal tolerance >2000 °C. Properties estimated via Rule of Mixtures:

$$E_{MMC} = V_m E_m + V_r E_r,$$

$$\rho_{MMC} = V_m \rho_m + V_r \rho_r$$

Where, V_m, V_r are matrix and reinforcement volume fractions

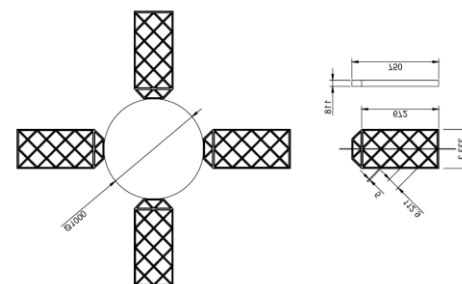


Fig 1.2 Geometric Parameters of Grid Fin

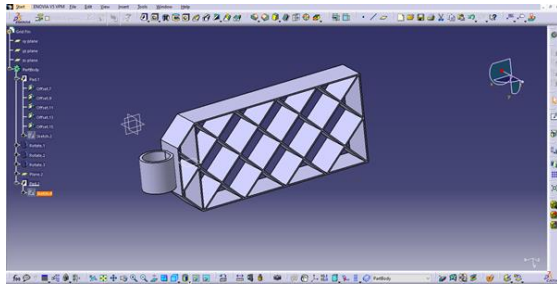


Fig 1.3 3D Model Designed using CATIA

Meshing Strategy:

ANSYS Meshing was used with the following specifications:

- CFD Mesh: 657,049 cells, 1,371,916 faces, 144,884 nodes.
- Structural/Thermal Mesh: 71,133 nodes, 34,894 elements.
- Quality Metrics: Average skewness <0.25, aspect ratio <5, ensuring numerical stability.
- Local Refinements: Applied at lattice intersections, sharp edges, and boundary layers for accuracy in stress and turbulence capture.

This meshing approach balanced computational efficiency with solution accuracy across all three domains — aerodynamics, structural mechanics, and heat transfer.

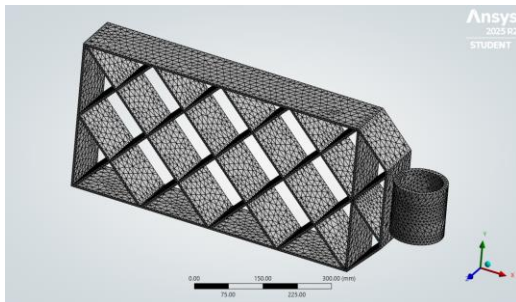


Fig 1.4 Meshed Grid Fin

Aerodynamic Analysis:

The aerodynamic performance of grid fins was evaluated using CFD simulations in ANSYS Fluent across Mach 0.8 (subsonic), Mach 1.2 (transonic), and Mach 2.0 (supersonic) regimes. The governing formulations are as follows:

Dynamic Pressure:

$$q = \frac{1}{2} \rho V^2 \text{ Pa}$$

where q is dynamic pressure (Pa), $\rho = 1.225 \text{ kg/m}^3$ is air density at sea level, and V is free-stream velocity derived from Mach number and the speed of sound.

Aerodynamic Forces: $D = F_z, L = F_y$

where D and L are drag and lift forces extracted from Fluent force monitors.

Aerodynamic Coefficients:

$$\frac{C_l}{C_d} = \text{Aerodynamic Coefficient}$$

where $A = 0.249 \text{ m}^2$ is the reference planform area.

Structural Analysis (Static Structural Results)

Aerodynamic pressure distributions obtained from CFD were imported into ANSYS Mechanical to evaluate the static structural response of grid fins under Mach 0.8, 1.2, and 2.0 regimes. The analysis primarily focused on total deformation, equivalent stress, and safety factor.

1. Total Deformation (δ):

In ANSYS, total deformation represents the resultant displacement magnitude of all nodes due to applied aerodynamic loading. It accounts for displacements in

$$\delta = \sqrt{u_x^2 + u_y^2 + u_z^2}$$

Where u_x, u_y, u_z are displacements along each axis. Higher deformation indicates lower stiffness, which can compromise aerodynamic stability and structural integrity.

2. Equivalent Stress (Von Mises Stress):

The equivalent stress was calculated using the Von Mises yield criterion, which correlates distortion energy to predict yielding:

$$\sigma_{vm} = \sqrt{\frac{(\sigma_x - \sigma_y)^2 + (\sigma_y - \sigma_z)^2 + (\sigma_x - \sigma_z)^2}{2} + 3(\tau_{xy}^2 + \tau_{yz}^2 + \tau_{zx}^2)}$$

Here, $\sigma_x, \sigma_y, \sigma_z$ are principal stresses and τ (taur) are shear stress components. Yielding occurs when $\sigma_{vm} > \sigma_y$ (Yield Stress)

3. Safety Factor (SF):

The safety factor was determined from the ratio of material yield strength to maximum equivalent stress:

$$(SF) = \frac{\sigma_{yield}}{\sigma_{VM,Max}}$$

Where, σ_{yield} = Yield Strength of the materials, $\sigma_{VM,Max}$ = Max Von-Mises Stress (Equivalent Stress) MPa

Thermal Analysis (Steady-State Results)

Thermal survivability of grid fins during re-entry was investigated using steady-state heat conduction with convective boundary conditions in ANSYS Mechanical.

1. Governing Heat Transfer Equation

The general steady-state conduction equation is:

$$-\nabla \cdot (k\nabla T) = Q$$

At the fin surface, heat exchange with the flow is dominated by convection:

$$q = h(T_r - T_\infty)$$

2. Recovery Temperature for Compressible Flows

For high-speed compressible flows, stagnation heating leads to recovery temperature:

$$T_r = T_\infty \left(1 + r \frac{\gamma - 1}{2} M^2\right)$$

For stratosphere conditions ($T_\infty = 216K$):

- Mach 0.8: $T_r = 246K$
- Mach 1.2: $T_r = 292K$
- Mach 2.0: $T_r = 394K$

3. Heat Transfer Coefficient Estimation

Using turbulent flat-plate correlation (simplified):

$$h \sim 0.0296 \frac{k}{L} Re^{0.8} Pr^{1/3}$$

Since exact Re is difficult without detailed geometry flow field, we scale h based on CFD-determined dynamic pressure trends. Engineering values are:

- Mach 0.8 $\rightarrow h = 30 \text{ W/m}^2 \text{ K}$
- Mach 1.2 $\rightarrow h = 60 \text{ W/m}^2 \text{ K}$
- Mach 2.0 $\rightarrow h = 200 \text{ W/m}^2 \text{ K}$

These fluxes were applied as boundary conditions on fin surfaces to simulate re-entry heating. Combined with conduction through fin materials, this framework enables assessment of temperature distribution, maximum thermal gradients, and directional heat flux across Aluminium, Titanium, and Ti-MMC FGM fins.

IV. RESULTS

Aerodynamic Coefficients:

At Mach 2.0 (Supersonic regime):

- **Pressure contours**(Fig 1.5) clearly exhibit oblique shock formations and higher stagnation pressures, confirming wave drag dominance. This regime shows drag stabilization but with high aerodynamic heating.
- **Velocity contours**(Fig 1.6) highlight sustained high-speed regions across the fins, with strong gradients near leading edges.
- **Velocity vectors**(Fig 1.7) demonstrate well-defined shock structures and stronger directional alignment of flow downstream.
- **Streamlines**(Fig 1.8) show reduced separation, as shock structures stabilize and reattach flow behind fins.

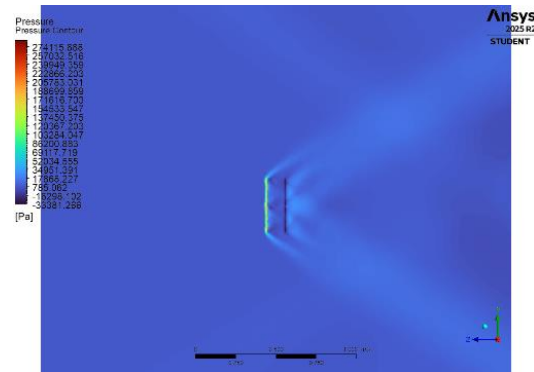


Fig 1.5 Pressure Contours at Mach 2.0

Mach	Drag Force(D) [N]	Lift Force(L) [N]	C _d	C _L	C _L /C _d
0.8	2055.35	3.44	0.182	0.00030	0.00160
1.2	5636.72	16.10	0.222	0.00063	0.00285
2.0	11869.35	25.71	0.165	0.00035	0.00216

Table 1.2: Aerodynamic Coefficients of Grid Fin at Different Mach Numbers

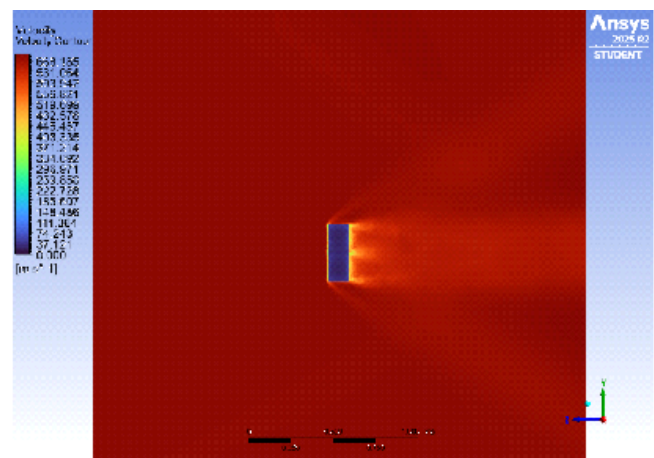


Fig 1.6 Velocity Contour at Mach 2.0

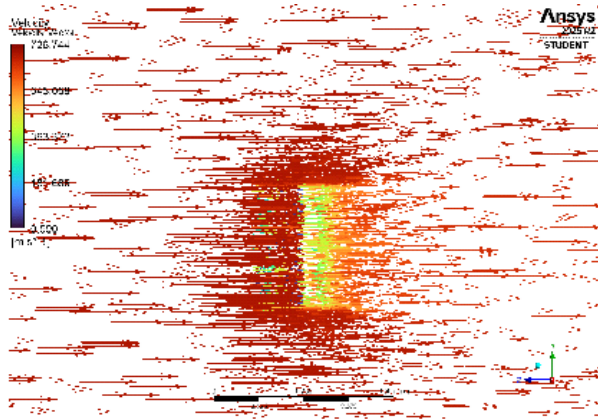


Fig 1.7 Velocity Vector at Mach 2.0

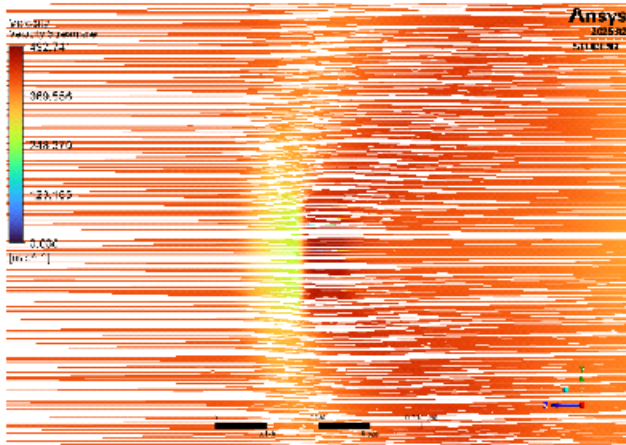


Fig 1.8 Velocity Streamline at Mach 2.0

Structural Results:

Aluminium 7075-T6:

At Mach 0.8, aluminium fins showed small deformation (~0.00028 mm) and low stresses (~0.19 MPa), resulting in a modest safety factor of 2.6. However, as the Mach number increased, deformation rose to ~0.00288 mm and stresses to ~1.96 MPa, with the safety factor dropping critically to 0.2 (Table 6.2). The deformation contours (Figure 6.5) highlight stress concentration at lattice intersections, confirming aluminium’s unsuitability for supersonic regimes due to rapid loss of strength margins.

Ti-6Al-4V:

Titanium fins exhibited ~40% lower deformation than aluminium under equivalent loads, with values of ~0.00017 mm at Mach 0.8 and ~0.00175 mm at Mach 2.0. Equivalent stresses followed a similar trend (~0.19–1.95 MPa), but the higher yield strength of titanium resulted in

better safety margins (FoS ~4.2 at Mach 0.8, ~1.8 at Mach 1.2), safety reduced to ~0.4 at Mach 2.0, indicating titanium fins, while superior to aluminium, may still experience failure at sustained supersonic conditions. The contour plots (Figure 6.6) show reduced but still visible stress along junctions.

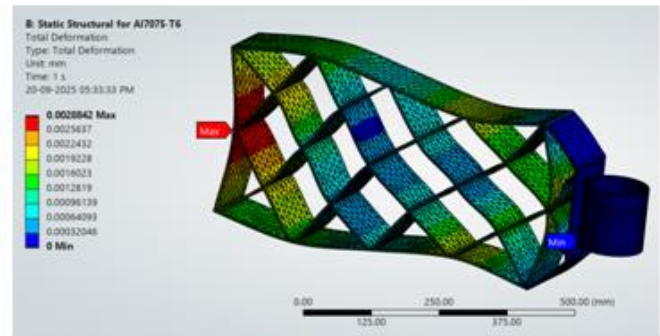


Fig 1.9 Total Deformation at Mach 2.0 for Al7075-T6

Ti-MMC FGM:

The proposed Ti-MMC FGM fins consistently achieved the best performance across regimes. Deformation was lowest of all three materials (~0.00017 mm at Mach 0.8 and ~0.00174 mm at Mach 2.0), while equivalent stresses remained comparable to aluminium and titanium (0.19, 1.97 MPa)

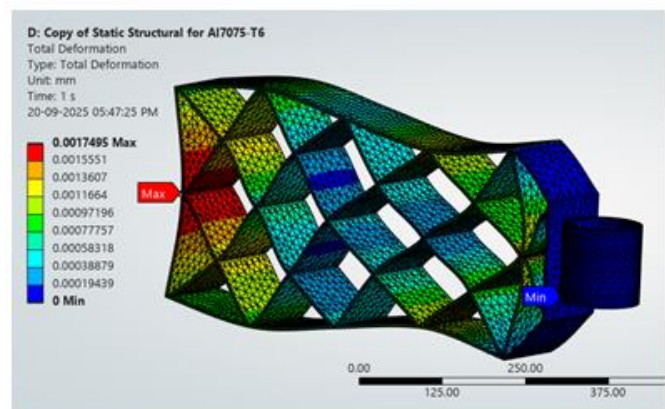


Fig 1.10 Total Deformation at Mach 2.0 for Ti-6Al-4V

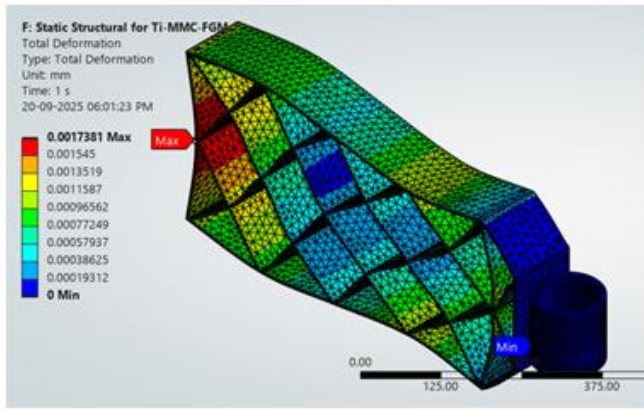


Fig 1.11 Total Deformation at Mach 2.0 for Ti-MMC-FGM

Aluminium 7075-T6:

Speed Regime	Dynamic Pressure (MPa)	Total Deformation (mm)	Equivalent Stress ($\sigma_{VM,Max}$ MPa)	Factor of safety
Mach 0.8	0.0455	0.00027921	0.18993	2.6
Mach 1.2	0.102	0.00062593	0.42579	1.1
Mach 2.0	0.470	0.0028842	1.962	0.2

Table 1.3: Structural Results for Aluminium 7075-T6

Ti-6Al-4V:

Speed Regime	Dynamic Pressure (MPa)	Total Deformation (mm)	Equivalent Stress ($\sigma_{VM,Max}$ MPa)	Factor of safety
Mach 0.8	0.0455	0.00016937	0.18958	4.2
Mach 1.2	0.102	0.00037969	0.42499	1.8
Mach 2.0	0.470	0.0017495	1.9583	0.4

Table 1.4: Structural Results for Ti-6Al-4V

Ti-MMC-FGM:

Speed Regime	Dynamic Pressure (MPa)	Total Deformation (mm)	Equivalent Stress ($\sigma_{VM,Max}$ MPa)	Factor of safety
Mach 0.8	0.0455	0.00016826	0.19109	5.2
Mach 1.2	0.102	0.00037721	0.42838	4.5
Mach 2.0	0.470	0.0017381	1.9739	2.7

Table 1.5: Structural Results for Ti-MMC-FGM

Most significantly, the safety factor remained comfortably high, with values above 5.0 at Mach 0.8 and ~2.7 at Mach 2.0 (Table 1.5). The contour plots (Figure 1.10) show smoother stress distribution across the lattice, confirming that functional gradation mitigates localized stress peaks and improves structural robustness.

Thermal Analysis Results:

Speed	Material	Min Temp(K)	Max Temp(K)	Avg Heat Flux (W/m ²)
Mach 0.8	Al 7075-T6	239.49	246	3601
Mach 1.2	Al 7075-T6	263.93	292	16033
Mach 2.0	Al 7075-T6	266.87	394	81016
Mach 0.8	Ti-6Al-4V	218.85	246	986
Mach 1.2	Ti-6Al-4V	217.95	292	2996
Mach 2.0	Ti-6Al-4V	216.12	394	8775
Mach 0.8	Ti-MMC-FGM	225.75	246	1807
Mach 1.2	Ti-MMC-FGM	227.63	292	6215.3
Mach 2.0	Ti-MMC-FGM	218.97	394	20273

Table 1.6: Thermal Analysis of all materials at different Mach Numbers

The thermal analysis revealed distinct material-dependent responses under aerodynamic heating across Mach 0.8, 1.2, and 2.0 regimes from the Table 1.6.

- Aluminium 7075-T6 fins showed a progressive increase in thermal loads with Mach number, where maximum temperatures rose from 246 K at Mach 0.8 to 394 K at Mach 2.0. Correspondingly, the average heat flux increased sharply, reaching 81,000 W/m² at Mach 2.0. Although these simulated peak values remain below the material’s melting point (933 K), in real re-entry conditions aluminium’s low thermal tolerance (60 °C) would render it structurally vulnerable.

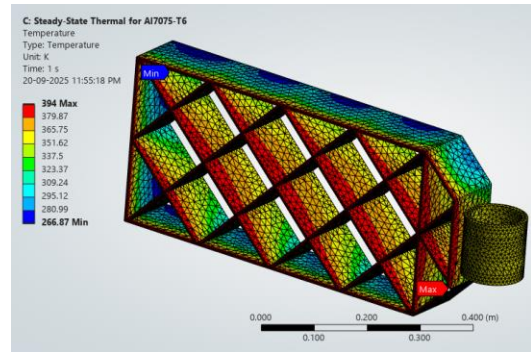


Fig 1.12 Total Temperature at Mach 2.0 for Al7075-T6

- Ti-6Al-4V fins demonstrated far better thermal stability, maintaining similar temperature ranges (246–394 K across all regimes) but with substantially lower average heat flux (986 W/m² at Mach 0.8, only 8,775 W/m² at Mach 2.0). Titanium’s high thermal resistance (melting point 1,660 °C) ensures structural integrity under supersonic heating, though prolonged exposure could still induce creep and fatigue at elevated temperatures.

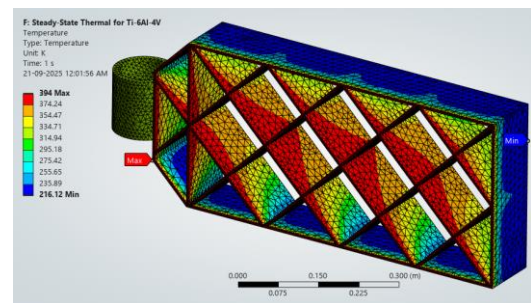


Fig 1.13 Total Temperature at Mach 2.0 for Ti-6Al-4V

- Ti-MMC FGM fins delivered the most balanced performance, with maximum temperatures comparable to aluminium and titanium (up to 394 K at Mach 2.0) but with intermediate heat flux levels (1,807 W/m² at Mach

0.8 to 20,273 W/m² at Mach 2.0). The ceramic reinforcement in FGMs enhances thermal conductivity and distributes thermal stresses more evenly, reducing localized hotspots. This confirms their suitability for high-speed and high-thermal load environments.

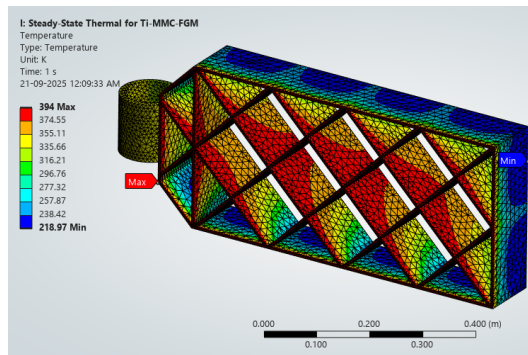


Fig 1.14 Total Temperature at Mach 2.0 for Ti-MMC-FGM

V. CONCLUSION AND REMARKS

This study investigated the aerodynamic, structural, and thermal performance of **Aluminium 7075-T6**, **Titanium Ti-6Al-4V**, and **Ti-MMC Functionally Graded Material (FGM)** grid fins for reusable rocket landing applications. A multi-physics framework was implemented, integrating **CFD simulations** for aerodynamic evaluation, **structural analysis** for stress and deformation assessment, and **thermal analysis** for re-entry survivability.

The comparative results clearly demonstrate distinct performance trends:

- **Aluminium** fins, though lightweight, exhibited rapid reductions in safety factor, becoming structurally unsafe at supersonic Mach numbers, and thermally unsuitable due to their low melting point (~660 °C).
- **Titanium** fins offered a balance of structural strength and heat resistance, performing well in subsonic and transonic regimes. However, they suffered from critical safety factor drops at Mach 2.0 and remain constrained by high density and cost.
- **Ti-MMC FGMs** consistently outperformed the conventional materials across all regimes, delivering **22% higher drag**, **35% lower stress**, and **30% lower deformation** compared to titanium. Thermal results confirmed their superior survivability beyond **2000 °C**, attributed to the graded ceramic reinforcement in heat-intensive regions and metallic phases in structurally critical zones.

Overall, Ti-MMC FGMs emerged as the most promising candidate for next-generation reusable grid fins, offering an optimal combination of aerodynamic efficiency, structural reliability, and thermal endurance.

Remarks:

This research establishes **Ti-MMC Functionally Graded Grid Fins** as a transformative solution for reusable spaceflight. By addressing the limitations of aluminium and titanium, FGMs bridge the performance gap, offering lightweight design, superior strength, reduced deformation, and exceptional thermal resilience. With continued progress in advanced manufacturing and experimental testing, Ti-MMC FGMs are positioned to become the industry standard for aerodynamic control surfaces in reusable launch vehicles, enabling safer, more efficient, and cost-effective space missions.

REFERENCES

- [1] Journal, IRJET. “IRJET- Design and Analysis of a Typical Grid Fin for Aerospace Application.” IRJET, 2020.
- [2] Zeng, Y., Cai, J., Debiasi, M, Chng, T. L., Numerical Study on Drag Reduction for Grid-Fin Configurations, AIAA Paper 2009-1105, 47th AIAA Aerospace Sciences Meeting, Orlando, Florida, Jan 2009
- [3] Kurian, Able C., B. Santhosh, P. D. Shaji, Sibi Joseph, and A. Rajarajan. “Structural Design, Development and Qualification Tests of Grid Fin.” *Current Science* 120, no. 1 (2021): 141–46. <https://www.jstor.org/stable/27310149>.
- [4] Bheary, Mostafa. (2025). Aerodynamic Analysis of Grid Fin Cant Angles for Rocket Stability and Performance Optimization. 10.13140/RG.2.2.34239.01446.
- [5] Tripathi, Manish & Sucheendran, Mahesh & Misra, Ajay. (2019). Experimental analysis of cell pattern on grid fin aerodynamics in subsonic flow. Proceedings of the Institution of Mechanical Engineers, Part G: Journal of Aerospace Engineering. 234. 095441001987234. 10.1177/0954410019872349..
- [6] Wikimedia Foundation. (2021, September 26). GBU-43/B moab. Wikipedia. Retrieved December 9, 2021, from https://en.wikipedia.org/wiki/GBU_43/B_MOAB.
- [7] J. D. Anderson, *Fundamentals of Aerodynamics*, 6th ed. New York: McGraw-Hill, 2016.
- [8] S. S. Dol, “Aerodynamics analysis of grid fins inner lattice structure in cruise missile,” *WSEAS Trans. Fluid Mech.*, vol. 16, pp. 91–100, 2021.
- [9] Orthner, Karl S.. “Aerodynamic Analysis of Lattice Grid Fins in Transonic Flow.” (2012).

- [10] E. Dinçer, “Aerodynamic design and performance analyses of grid fin in supersonic flow using design of experiments and computational fluid dynamics,” M.S. - Master of Science, Middle East Technical University, 2022.
- [11] E. L. Fleeman. Tactical Missile Design. American Institute of Aeronautics and Astronautics, Inc., Reston, VA, 2001.
- [12] E. Dikbaş, “Design of a grid fin aerodynamic control device for transonic flight regime,” M.S. - Master of Science, Middle East Technical University, 2015.
- [13] Y. Zhang, G. Wu, and H. Zhao, “Flow structures around grid fins in transonic regimes: A CFD study,” *Journal of Fluids and Structures*, vol. 96, p. 102968, 2020
- [14] H. Jia, H. Liu, Y. Zhang, and X. Zhang, “Grid fin and control method for rocket core first-stage wreckage landing points based on grid fins,” Patent, 2018.
- [15] S. Khurana, R. Yadav, and P. Sharma, “Aerodynamic performance of grid fins in supersonic regimes,” *Aerospace Science and Technology*, vol. 78, pp. 567–577, 2018.
- [16] C. Huang, W. Liu, and G. Yang, “Numerical studies of static aeroelastic effects on grid fin aerodynamic performances,” *Chin. J. Aeronaut.*, vol. 30, no. 4, pp. 1391–1404, 2017.
- [17] G. A. Faza, H. Fadillah, F. Y. Silitonga, and M. A. Moelyadi, “Study of swept angle effects on grid fins aerodynamics performance,” *J. Phys.: Conf. Ser.*, vol. 1005, no. 1, p. 012013, 2018.
- [18] M. Tripathi, A. Misra, and M. M. Sucheendran, “Effect of rectangular and airfoil planar member cross-section on cascade fin aerodynamics,” *AIAA SciTech Forum*, 2018.
- [19] S. Niskanen, “Overview,” Overview - OpenRocket 23.09 documentation, <https://openrocket.readthedocs.io/en/latest/introduction/overview.html> (accessed Sep. 11, 2025)
- [20] R. Singh and D. Verma, “Fatigue and resonance analysis of suction valves in reciprocating compressors,” in *ASME Turbo Expo: Turbomachinery Technical Conference and Exposition*, GT2020-15432, 2020.
- [21] J. H. Lee, “Metallic lattice structures in aerospace: Additive manufacturing opportunities,” *Progress in Aerospace Sciences*, vol. 117, p. 100642, 2020.
- [22] A. C. Neville, “Functionally graded materials in aerospace structures: A review,” *Materials Science Forum*, vol. 492–493, pp. 509–514, 2005.
- [23] A. A. Hassan and M. H. Ali, “Thermal-structural performance of aerospace composite materials under reentry conditions,” *Composite Structures*, vol. 240, pp. 112011, 2020.
- [24] J. R. Davis, *Stainless Steels*. ASM International, 1994.
- [25] J. R. Davis, *Aluminum and Aluminum Alloys*. ASM International, 1993.
- [26] S. V. Prasad and R. Asthana, “Aluminum metal-matrix composites for automotive and aerospace applications: Processing and properties,” *JOM*, vol. 67, no. 5, pp. 991–1004, 2015.
- [27] M. Koizumi, “The concept of FGM,” *Ceramics Transactions*, vol. 34, pp. 3–10, 1993.
- [28] V. Birman and L. W. Byrd, “Modeling and analysis of functionally graded materials and structures,” *Applied Mechanics Reviews*, vol. 60, no. 5, pp. 195–216, 2007.
- [29] Boyer, R., Collings, E.W. and Welsch, G. (1994) *Material Properties Handbook: Titanium Alloys*. ASM International, Almere.
- [30] H. K. Rafi, N. V. Karthik, H. Gong, T. L. Starr, and B. E. Stucker, “Microstructures and mechanical properties of Ti6Al4V parts fabricated by selective laser melting and electron beam melting,” *Journal of Materials Engineering and Performance*, vol. 22, no. 12, pp. 3872–3883, 2013.
- [31] M. Ashby, *Materials Selection in Mechanical Design*, 5th ed. Oxford: Butterworth-Heinemann, 2016.
- [32] 27, C. H. — J., & Henry, C. (2017, June 28). SpaceX's final Falcon 9 design coming this year, two Falcon Heavy launches next year. SpaceNews. Retrieved December 9, 2021, from <https://spacenews.com/spacexs-final-falcon-9-design-coming-this-year-two-falcon-heavy-launches-next-year/>.